Available online at www.sciencedirect.com

SciVerse ScienceDirect

Journal of the European Ceramic Society 32 (2012) 1175–1186

www.elsevier.com/locate/jeurceramsoc

A lifetime prediction method based on Cumulative Flaw Length Theory

D.N. Boccaccini [a], M. Maioli [b], M. Cannio [a,*], I. Dlouhy [c], M. Romagnoli [a], C. Leonelli [a], A.R. Boccaccini [d]

[a] *Dipartimento di Ingegneria dei Materiali e dell'Ambiente, Università di Modena e Reggio Emilia, Via Vignolese 905, 41100 Modena, Italy*
[b] *Dipartimento di Matematica, Via Campi 213/B, 41100 Modena, Italy*
[c] *Institute of Physics of Materials, ASCR, CZ-61662 Brno, Czech Republic*
[d] *Department of Materials Science and Engineering, University of Erlangen-Nuremberg, 91058 Erlangen, Germany*

Received 23 May 2011; received in revised form 12 November 2011; accepted 28 November 2011
Available online 23 December 2011

Abstract

Ultrasonic pulse velocity testing (UPVT) was carried out to perform non-destructive quality control of refractory plates. Used in conjunction with fracture mechanics, ultrasonic velocity measurements have proved a powerful technique for detecting, positioning and sizing internal voids and cracks in the samples, originated from the manufacturing process. Two cordierite-mullite refractory compositions exhibiting different microstructure and crack propagation behaviour were characterized through their lifetime during which they were subjected to thermal shock loading. In this paper, a new statistical method is proposed which allows to estimate the lifetime when the stress state that will be applied in service (loading) and the scattering of the ultrasonic velocity data in the as-received state are known. Since this lifetime prediction method is based on a non-destructive technique, it could be implemented into a code in an automatic quality control device for continuous lifetime estimation. The correlation between crack propagation behaviour and thermal shock resistance is discussed and semi-empirical models were developed to predict the service life of refractory plates from the measured values of ultrasonic velocities on as-received samples.

Keywords: Non-destructive evaluation; Residual stress; Thermal shock resistance; Mullite; Cumulative Flaw Length Theory

1. Introduction

A variety of strength-degrading flaws usually introduced during the initial stages of powder processing can lead to unacceptable low mechanical strength of high temperature ceramic materials. Impurities in the starting material components (powder, sintering aids, binders) and agglomerates formed during powder processing are two examples of strength-degrading flaws. Internal cracks not only limit the ultimate strength of these materials but also increase the variability of measured strength values giving rise to low reliability (low Weibull modulus). A primary objective of statistical fracture theories is to predict the probability of failure of a component for an arbitrary stress state when the failure statistics is known. A new approach, entitled "Cumulative Flaw Length Theory (CFLT)", has been developed for the case of macroscopically homogeneous isotropic materials containing randomly oriented microcracks uniformly distributed in locations under non uniform multiaxial stresses.[1] The theory estimates the failure probability based on the non-destructive measurement of the velocity of propagation of ultrasonic waves through the material. Ultrasonic testing can provide the information required by fracture mechanic approaches, while fracture mechanics incorporates in turn the targets for the performance of ultrasonics. An increasing number of recent investigations has demonstrated the convenient use of ultrasonic velocity measurements to assess fracture properties of ceramic materials.[2–6] The complete description of the CFLT approach has been presented in a previous investigation.[1] Comparing with existing approaches to failure probability estimation in ceramic materials, which are mainly based on data from destructive tests, CFLT presents the unique advantage that failure probability assessment is achieved from parameters determined by non-destructive characterization.[1] This fact could enable its use not only in the stage of materials design, but also to monitor the expected increase of failure probability during the materials service life. In this novel approach, the function representing the

* Corresponding author.
E-mail address: maria.cannio@unimore.it (M. Cannio).

0955-2219/$ – see front matter © 2011 Elsevier Ltd. All rights reserved.
doi:10.1016/j.jeurceramsoc.2011.11.042

Nomenclature

CFLT	Cumulative Flaw Length Theory
CN	chevron notch technique
F_{max}	maximum load
ith	path of the ultrasonic wave
K_{IC}	fracture toughness
L	length of the path
LPT	lifetime prediction time
$N_V(\sigma)$	the crack density function
$N_v(\lambda)$	as the relative frequency
NDE, NDT	non-destructive evaluation
$(\Delta P_f)_i$	probability of failure
P_f	failure probability
P_s	survival probability
$\sum_i (\Delta P_f)_i$	risk of failure
$(\Delta P_s)_i = 1 - (\Delta P_f)_i$	survival probability
Y^*_{min}	geometrical compliance function
u	ultrasonic velocity
UPVT	ultrasonic pulse velocity testing
λ	cumulative flaw length
λ_1	mode value of cumulative flaw length
$\Omega(\Sigma, \lambda)$	solid angle
σ	flexural strength

number of cracks per unit volume is estimated from histograms of ultrasonic velocity measurements.[1,7] This function is used without additional assumptions to determine the probability of fracture under arbitrary stress conditions.

Thus, CFLT enables determination of the flaw density function and the failure probability based on the measurement of ultrasonic velocity in ceramic materials. In the present study, a new approach is proposed that, based on the results obtained from CFLT for as-received samples, allows the lifetime estimation of a component when the stress state in service and the scattering of the ultrasonic velocity values in as-received state are known. In thermally shocked refractory materials, this theory is proposed as a method to determine the number of thermal shock cycles that the materials can withstand without complete failure. Two different cordierite-mullite high temperature ceramic materials were characterized to provide experimental evidence in support of the theoretical predictions. Empirical models of service life were obtained counting the number of industrial thermal cycles performed by a statistically significant number of specimens. The good correlation obtained between theoretical curves of lifetime prediction and the empirical curves determined from experimental data seems to confirm the robustness of the proposed methodology.

1.1. Ultrasonic propagation and CFLT

In the case of the refractory materials here investigated, the ultrasonic velocity varies from 2000 to 3000 m/s in the as-received state.[7] In the presence of cracks, the ultrasonic waves generated by the transmitter transducer cross the boundary of the crack reaching the receiving transducer while the waves crossing the crack travelling through the air undergo a remarkable decrease of amplitude and a delay in time leading to a final loss of signal. For these reasons, thermally shocked materials show a significant decrease of ultrasonic velocity values, since the ultrasonic waves must contour the cracks before reaching the receiving transducer (in the case of the materials here investigated, after 400 thermal shock cycles, the ultrasonic velocity is close to 1000 m/s).[7] Hence ultrasound can be considered sensitive to detect the onset of cracks ranging from about 500 μm and its further development when materials are subjected to external stresses. These simple physical phenomena occurring in an UPVT measurement have been widely reported in literature[5] and represent the base of our hypothesis to build a mathematical model, linking crack lengths to ultrasonic velocity.

1.2. Fracture mechanics and CFLT

The application of linear fracture mechanics (LEFM) models to the ceramic materials here studied is questionable because the materials are not monolithic ceramics, but highly heterogeneous refractory materials with remarkable r-curve behaviour, as extensively demonstrated in literature.[8–12] Furthermore the degradation of the materials is generated from thermal stresses (not mechanical loading) as the samples are subjected to the thermal shocks of the fast firing cycles. The materials are tested under real service life conditions, e.g. cracks propagate macroscopically due to thermal stresses under thermal shock conditions. In practice, the materials fail due to thermal fatigue after a limited number of cycles. To predict this failure behaviour, it is generally not possible to use linear elastic fracture mechanics due to the fact that the coarse grained, porous material shows a dissipative mechanical behaviour. In this investigation, actual industrial samples of large dimensions (540 mm × 120 mm) are considered, hence the "size effect" is relevant, as extensively demonstrated in literature.[13]

The study of refractory structures over the past twenty years has shown that refractory material behaviour is highly non-linear with time and temperature.[8–12] This is due to the formation of a so-called "fracture process zone" in the wake of the crack tip. In this fracture process zone the crack faces are not completely stress free as assumed in the LEFM theory, but still have some interaction due to the bridging and sliding of grains in this region. The size of the process zone, compared with the size of the structure, determines the influence of the process zone on the overall mechanical properties. For quasi-brittle materials, the size of the process zone is relatively large and cannot be neglected. These materials show a macroscopic quasi-brittle failure behaviour due to the additional energy dissipation in the process zone. The transition from brittle to quasi-brittle failure behaviour is a combined structural and material process.

Hasselman[14] established the first approach to determine the resistance to crack initiation and crack propagation in refractory materials almost 40 years ago. In case of highly heterogeneous materials (not monolithic) considered in this study, the lifetime does not depend on the resistance to crack initiation but on the

resistance of crack propagation, as determined by Hassemann's parameter Rst.[14] It is well known in refractory industry that a refractory material with early crack initiation most of the times shows delayed crack propagation.[7] The failure of refractory plates considered in this study is due to a one single macroscopic crack propagating in the transversal direction of the plates. In this context, the application of LEFM models to study this macroscopic crack (larger than 0.5 mm) in heterogeneous materials with remarkable r-curve behaviour is not viable. Relevant results have been achieved and verified with experimental data from the determination of the macroscopic crack length using ultrasonic velocity testing.[7] The cumulative flaw length value calculated by Eq. (11) is a close form function that approaches the real critical crack length value as the crack length increases (the one single macroscopic crack propagating in the transversal direction of the plates).

The lifetime can be monitored studying the crack growth (the characteristic S-curve of the materials). The length of this macroscopic critical crack and its growth with increasing thermal shock cycles (lifetime) can be easily monitored by ultrasonic pulse velocity testing (UPVT). UPVT has a long tradition of application in refractory industry. The present study provides the theoretical background to calculate from ultrasonic velocity data the dimension of the macroscopic critical crack length and from its velocity of propagation (under real time testing) the lifetime of the material. Once an statistically relevant number of samples has been tested and recorded (100 in this case), it is possible to build a model to predict lifetime of samples of the same material in the as-received state and that will be applied under the same service life conditions.

2. Description of the theoretical approach

2.1. Determination of failure probability

Let $(\Delta P_f)_i$ be the probability of failure at some point of the ith path of the ultrasonic wave through the material.

Let

$$(\Delta P_s)_i = 1 - (\Delta P_f)_i \tag{1}$$

be the corresponding survival probability, where P_f and P_s are the failure and the survival probability, respectively. Thus P_s can be written as:

$$P_s = \prod_i (\Delta P_s)_i = \prod_i (1 - (\Delta P_f)_i) \cong \prod_i e^{-(\Delta P_f)_i} \tag{2}$$

$$P_s = e^{(-\sum_i (\Delta P_f)_i)} \tag{3}$$

where $\sum_i (\Delta P_f)_i$ can be regarded as the measurement of the risk of failure.

The potential causes of fracture are the cumulative lengths of flaws along the path, where a path of length L can be defined as the distance travelled through the material by the ultrasonic wave between the two piezoelectric sensors. Thus it is possible to associate a *cumulative length of flaws* to each path. The evaluation of such length for each line path can be experimentally performed by measuring the ultrasonic propagation velocity.

We define $N_v(\lambda)$ as the relative frequency of paths with cumulative length of flaws less than or equal to λ, per unit of volume, where λ is the cumulative flaw length.

The function representing the number of cracks per unit volume is estimated based on the histograms of ultrasonic velocity measurements.[1] This function is used without additional assumptions to determine the probability of fracture under an arbitrary stress condition. In other words, $N_v(\lambda)$ determines a probability distribution. Then the probability for a flaw to have a cumulative length in $[\lambda,\lambda + d\lambda]$ is:

$$\Delta V \cdot N'_V(\lambda) d\lambda = \Delta V \cdot \frac{dN_V(\lambda)}{d\lambda} d\lambda \tag{4}$$

If Σ denotes the applied stress, we can also consider the solid angle $\Omega(\Sigma, \lambda)$ which is determined by directions along which the stress causes fracture due to flaws of length λ or higher, according to corresponding fracture mechanics criteria.[15,16]

Then the probability that a path in volume ΔV has a cumulative flaw length in the range $[\lambda,\lambda + d\lambda]$ with stress orientation in $\Omega(\Sigma, \lambda)$ is:

$$\Delta V \cdot N'_V(\lambda) d\lambda \cdot \frac{\Omega(\Sigma, \lambda)}{4\pi} \tag{5}$$

The probability that at least one failure event will occur along a path with cumulative flaw length λ_1 will be:

$$P_f = \int dV \int_{\lambda_1}^{+\infty} \frac{dN_V(\lambda)}{d\lambda} d\lambda \cdot \frac{\Omega(\Sigma, \lambda)}{4\pi} \tag{6}$$

where λ_1 is the mode value.

Then the survival probability, P_s, for the length $\geq \lambda_1$ can be written as:

$$P_s = \exp\left[- \int dV \int_{\lambda_1}^{+\infty} \frac{dN_V(\lambda)}{d\lambda} d\lambda \cdot \frac{\Omega(\Sigma, \lambda)}{4\pi} \right] \tag{7}$$

or equivalently, the failure probability in paths with cumulative flaw length $\geq \lambda_1$ is:

$$P_f = 1 - \exp\left[- \int dV \int_{\lambda_1}^{+\infty} \frac{dN_V(\lambda)}{d\lambda} d\lambda \cdot \frac{\Omega(\Sigma, \lambda)}{4\pi} \right] \tag{8}$$

From the experiments of ultrasonic velocity measurement, if velocities v are measured along a linear path of length L, then the corresponding cumulative flaw length (λ) is given by:

$$\lambda = \lambda(v) = L\left(\frac{v_0}{v} - 1\right) \tag{9}$$

where v_0 is the maximum value of velocity in the measured sample. Indeed, if $v_0 = L/t_0$ (i.e. t_0 is the shortest transit time) then the generic velocity can be written as $v = L/t(v)$; hence $t(v) = L/v$ and

$$v_0 = \frac{L + \lambda}{t(v)} = \frac{L + \lambda}{L/v} \tag{10}$$

Finally λ can be written as:

$$\lambda = v_0 t(v) - L = v_0 \frac{L}{v} - L = L\left(\frac{v_0}{v} - 1\right) \tag{11}$$

Table 1
Chemical composition of the investigated AR002 and CONC refractory plates.

Sample	SiO_2	Al_2O_3	CaO	MgO	Na_2O	K_2O	Fe_2O_3	TiO_2	Others	Total
AR002	44.32	42.47	0.38	5.58	0.32	0.74	1.42	0.45	4.32	100.00
CONC	46.86	37.91	0.00	7.89	0.00	0.58	1.38	0.61	4.77	100.00

2.2. Lifetime prediction theory (LPT)

In thermally shocked materials, the lifetime is quantified by the number of thermal shocks that a component can survive without failure. Given the number of thermal cycles (i.e. lifetime) as a function of the cumulative flaw length, $n = n(\lambda)$, and the probability density $f(\lambda)$ obtained experimentally for an as-received component by the ultrasonic velocity method, the expected value of the lifetime of such a material is:

$$E(n) = \int_0^{+\infty} n(\lambda) f(\lambda) d\lambda \tag{12}$$

The variance and standard deviation of this value are:

$$Var(n) = \int_0^{+\infty} (n(\lambda) - E(n))^2 f(\lambda) d\lambda \tag{13}$$

$$\mathrm{SD} = \sqrt{Var(n)} \tag{14}$$

respectively.

Such parameters can be estimated by means of the following approach.

First, we single out short subintervals $[\lambda_{i-1}, \lambda_i]$ whose union is the whole range of the lengths according to:

$$[0, \lambda_{\max}] = \bigcup_{i=1}^{K} [\lambda_{i-1}, \lambda_i] \tag{15}$$

with corresponding mean number of cycles $n_1, \ldots, n_K$. These mean numbers $n_1, \ldots, n_K$ can be determined from a representative number of components (observed units) of the same material in as-received state.

Each number of cycles n_i is then weighted by means of the corresponding relative frequency f_i of the flaw lengths belonging to $[\lambda_{i-1}, \lambda_i]$, i.e. the number of measured values of λ in the interval $[\lambda_{i-1}, \lambda_i]$ divided by the λ sample dimension. Therefore the sample mean, the sample variance and the standard deviation are:

$$\bar{n} = \sum_{i=1}^{K} n_i f_i \tag{16}$$

$$Var(n) = \mathrm{SD}^2 = \sum_{i=1}^{K} (n_i - \bar{n})^2 f(\bar{\lambda}_i) \tag{17}$$

$$\mathrm{SD} = \sqrt{Var(n)}, \quad \text{respectively.} \tag{18}$$

3. Experimental

3.1. Samples and test method

One hundred plates of two refractory materials, labelled AR002 and CONC, with identical dimensions (520 mm × 340 mm × 12 mm) were investigated. Table 1 reports the chemical composition of the AR002 and CONC plates (in wt%) obtained by ICP analysis (Varian, Liberty 200), while Table 2 summarizes the basic properties of these materials, as measured in previous studies.[7]

3.2. Ultrasonic pulse velocity (UPVT) measurements

For each refractory plate, measurements of ultrasonic pulse velocity through the length and thickness on direct transmission disposition were performed. A commercial ultrasonic testing instrument of transmission type (PUNDIT *plus* PC1006, CNS Farnell Ltd., Hertfordshire, England) was used to evaluate each refractory sample. The instrument consists of a pulse generator and a timing circuit coupled to two transducers (220 kHz) that were positioned manually at opposite ends (in through thickness direction of 12 mm dimension and in longitudinal direction of 520 mm dimension) of each test plate. Each transducer had a 1.6 mm thick rubber tip to overcome measurement problems due to the roughness of the refractory surface. Each test was run at least 5 times to determine the ultrasonic velocity with sufficient statistical relevance. The measurements were performed on the same batch of refractory plates in the as-received condition.

3.3. Thermal shock experiments

The performance of the refractory plates was tested on-duty in industrial whiteware kilns following the thermal treatment

Table 2
Physical, thermal and mechanical properties of the as-received AR002 and CONC refractory materials.[7]

Parameter	AR002	CONC
Bulk density, ρ (g/cm^3)[a]	2.08	1.91
Thermal expansion coefficient, α (25–1250 °C) ($K^{-1} \times 10^{-6}$)	3.06	2.49
Apparent porosity (%)	24	28
Young's modulus, E, Impulse Excitation Technique (I.E.T.) (GPa)	21.5	15.7
Poisson's ratio, μ, Impulse Excitation Technique (I.E.T.)	0.16	0.16
Three point bending strength, σ (MPa)	26	22
Fracture toughness, K_{IC} (MPam$^{1/2}$)	0.50	0.42

[a] GeoPyc 1360 Micromeritics, Norcross, GA 30093-1877, USA (reproducibility ±1.1%).

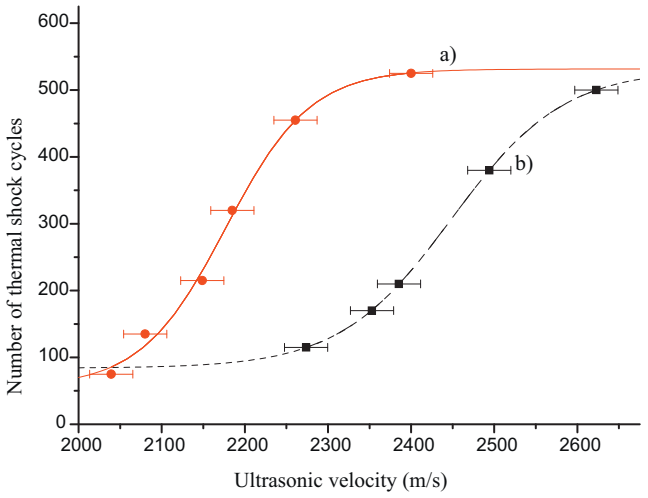

Fig. 1. Number of industrial thermal cycles as function of ultrasonic velocity measured in as-received state through the length for (a) CONC and (b) AR002 materials.

employed in fast firing cycles (maximum temperature between 1250 and 1275 °C). The term "thermal shock" is used throughout the text in agreement with the literature on refractory materials. Hence, the number of thermal shock experiments hereafter considered corresponds to the number of fast firing cycles carried out on the refractory plates. In total 100 refractory plates of each composition were marked and followed during all their service life. In many refractory plates, even if cracks were already visible after few thermal cycles, the propagation through the transversal direction of the plates occurred in relatively slow mode (particularly evident for CONC material[7]).

3.4. Fracture toughness determination

Fracture toughness data of selected samples before and after industrial thermal cycles were obtained by the chevron notch (CN) technique at room temperature. The specimen geometry employed in this test was a bar with dimensions $W = 4$ mm, $B = 3$ mm, $l = 22$ mm, where W = thickness, B = width and l = length, respectively. Chevron notches with angles of 90° were cut using a thin diamond wheel. The specimens were loaded in three-point bending configuration with rollers span of 16 mm at a constant cross-head speed of 0.01 mm/min. Graphs of load versus deflection were recorded and the fracture toughness was calculated from the maximum load (F_{max}) and the corresponding minimum value of geometrical compliance function (Y^*_{min}) using the following equation[7]:

$$K_{Ic} = \frac{F_{max}}{BW^{1/2}} Y^*_{min} \quad (19)$$

The calculation of the function Y^*_{min} for chevron notched bending bars was based on Bluhm's slice model,[17] as reported elsewhere.[7] The chevron-notch depth (a_0) was measured from optical micrographs of fractured specimens.

4. Results

4.1. Relation between as-received ultrasonic velocity values and number of thermal shock cycles

Fig. 1a and b shows the average number of thermal cycles (N), considered in this study as a quantitative measure of the materials service life, as function of ultrasonic velocity (v) values measured on the plates in the as-received condition (following the length path of the refractory plates) for CONC and AR002 materials, respectively. Error bars showing minimal and maximal measured values are also reported. In both materials, it is evident that service life of the refractory plates, measured as the number of cycles that the materials can withstand without fracture, increases with increasing values of ultrasonic velocity.

In the next paragraphs we explain how these N versus as received v curves can be transformed into N versus λ curves by applying CFLT approach (Fig. 2A and B) and how it is

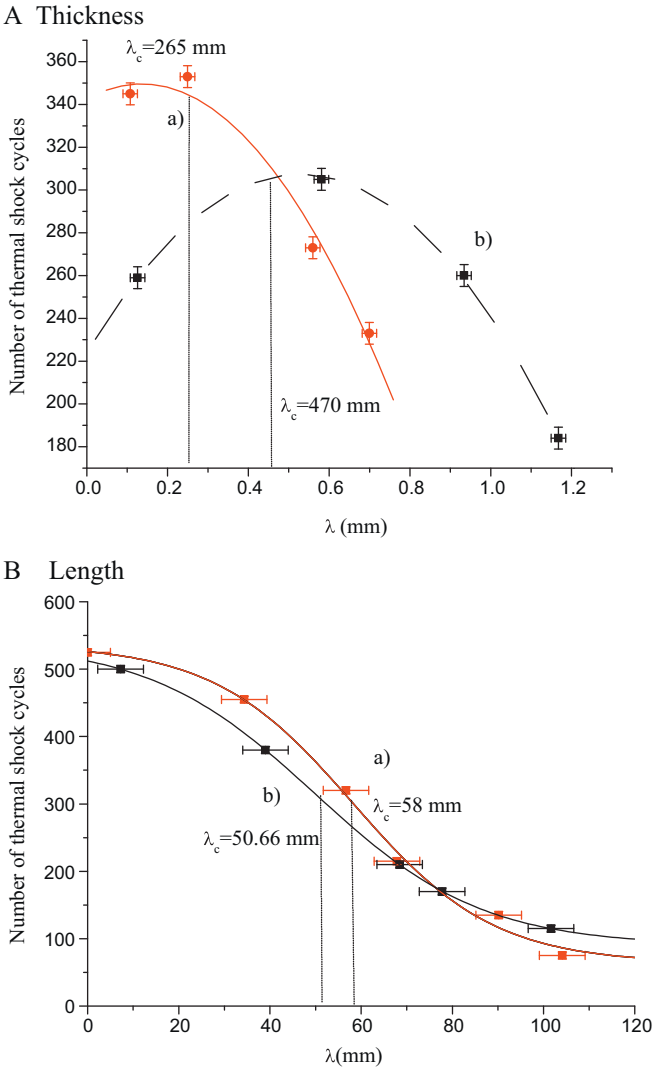

Fig. 2. Crack length values determined by CFLT as function of the service life of the refractory materials, for ultrasonic velocity values measured in as-received state through thickness (A) for (a) CONC and (b) AR002 materials, and through the length (B) for (a) CONC and (b) AR002 materials.

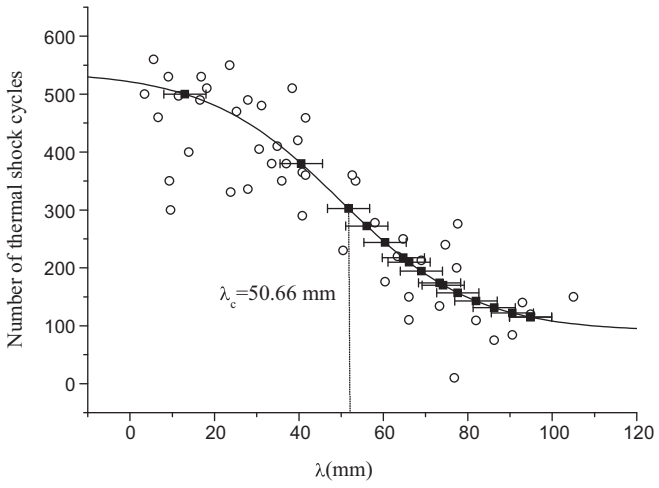

Fig. 3. Comparison between real and predicted by LPT method lifetime values for AR002 material.

possible to calculate the critical flaw length from these material characteristic curves (Fig. 3, Section 4.3).

4.2. Prediction of service life: case study of LPT

LPT was applied for the same lot of samples, i.e. AR002 and CONC refractory materials following the statements explained in Section 2.2. For lifetime prediction, firstly the paths (λ_i) corresponding to ultrasonic velocity values of a representative number of components (observed units) of the same material in as-received state must be calculated using Eq. (11). In other words, the curves reported in Fig. 1 representing number of thermal shock cycles (N) against ultrasonic velocity measured in the as-received state are transformed in N versus flaw length curves (λ) by applying Eq. (11). Table 3 reports an example of application of this approach, where the frequency and relative frequency of number of cycles for a representative number of samples of the same material (n_i) falling into the $[\lambda_{i-1}, \lambda_i]$ subinterval are listed in columns 2 and 3. Moreover the mean value of the number of cycles for each subinterval is reported in column 4, and finally, the relative frequencies of cumulative flaw lengths calculated by Eq. (11) from the ultrasonic velocity values obtained after careful screening measurements of the new component are included in column 5.

For understanding of the methodology, we include the detailed description of the approach, as follows.

The theoretical approach explained in Section 2.2 should be followed in this order:

(a) Divide the interval $[0, \lambda_{max}]$ into short subintervals of paths $[\lambda_{i-1}, \lambda_i]$ (column 1 of Table 3).
(b) For each of these subintervals calculate the mean number of cycles $n_1, \ldots, n_K$, together with the relative frequencies for a representative number of components (observed units) of the same material in as-received state. In the case studied here, 50 refractory samples of both compositions, AR002 and CONC, were marked and monitored during all their service lives. The results of the mean values of number of cycles n_i against the cumulative flaw lengths (λ) are shown in Fig. 2B, defining an S-like curve which could be the characteristic lifetime trend of refractory materials when subjected to thermal shock conditions (i.e. column 2, 3 and 4 of Table 3). Moreover it is suggested that this S-like curve could represent a characteristic materials curve, giving information for fracture mechanics studies, as discussed further below (Section 5.1).
(c) Once this S-like curve is defined for a specific material (cordierite-mullite refractory plates in our case), the lifetime of for a new component of the same material, with the same geometry and that will work under the same service life conditions, can be predicted, as follows.

Table 3
Example of LPT method for prediction of the service life of ceramic components.

Cumulative flaw length calculated from ultrasonic velocity	F_i and f_i of n_i for a representative number of samples of the same material in the range $[\lambda_{i-1}, \lambda_i]$		Mean number of cycles in the $[\lambda_{i-1}, \lambda_i]$ subinterval	f_i of λ_i for a new component in the range $[n_{i-1}, n_i]$
$[\lambda_{i-1}, \lambda_i]$	F_i	f_i	n_i	f_i
[0, 0.25]	5	0.056	300	0.04
[0.25, 0.75]	8	0.089	156.66	0.07
[0.75, 1.25]	10	0.112	450	0.13
[1.25, 1.75]	29	0.325	258	0.0324
[1.75, 2.25]	32	0.359	261	0.359
[2.25, 2.75]	4	0.045	353	0.045
[2.75, 3.25]	1	0.011	120	0.011
Predicted lifetime of the new component $\bar{n} = \sum_{i=1}^{K} n_i f_i$	–	–	–	**200.72**

The same short subintervals of paths $[\lambda_{i-1}, \lambda_i]$ singled out previously are weighted by means of the corresponding relative frequency f_i of the flaw lengths belonging to $[\lambda_{i-1}, \lambda_i]$, i.e. the number of measured values of λ in the interval $[\lambda_{i-1}, \lambda_i]$ divided by the λ sample dimension (column 5 of Table 3). Therefore the sample mean lifetime can be calculated using Eq. (16).

A new lot of fifty plates of AR002 and fifty plates of CONC material with identical dimensions (520 mm × 340 mm × 12 mm) were marked and monitored during all their service lives to validate the model. For each refractory plate, measurements of ultrasonic pulse velocity through the length and thickness in as-received state were performed. Fig. 3 shows the predicted mean lifetime values for ultrasonic velocity data measured through the length for AR002 material and the points representing the real lifetimes of this second lot of 50 samples used to validate the approach. Thus the real lifetime of these new 50 samples (dots) and the predicted mean lifetime (curve) can be compared in Fig. 3. The predicted mean lifetime values have been theoretically determined by applying the LPT approach as explained above. It is clear that even if significant differences exist between the absolute values of predicted lifetime with the real values, after 250 thermal shock cycles, from 17 broken samples, 16 samples belong to the lot of samples marked as critical before thermally shocking them, since they had λ values higher than critical (λ critical = 50.66 mm). The determination of these critical values is shown in the next section.

4.3. Assessment of the goodness of fitting between the semi-empirical theoretical model and experimental data

Kolmogorov–Smirnov (K–S) and *T*-tests with the calculation of the relative error have been used to validate the "goodness" of fitting of the model with the experimental data.

The comparison between the theoretical model and experimental data is reported in Fig. 3 for AR002 material. The sigmoidal curve was derived from a polynomial fitting of the mean values obtained as explained in Section 2.2 and also in

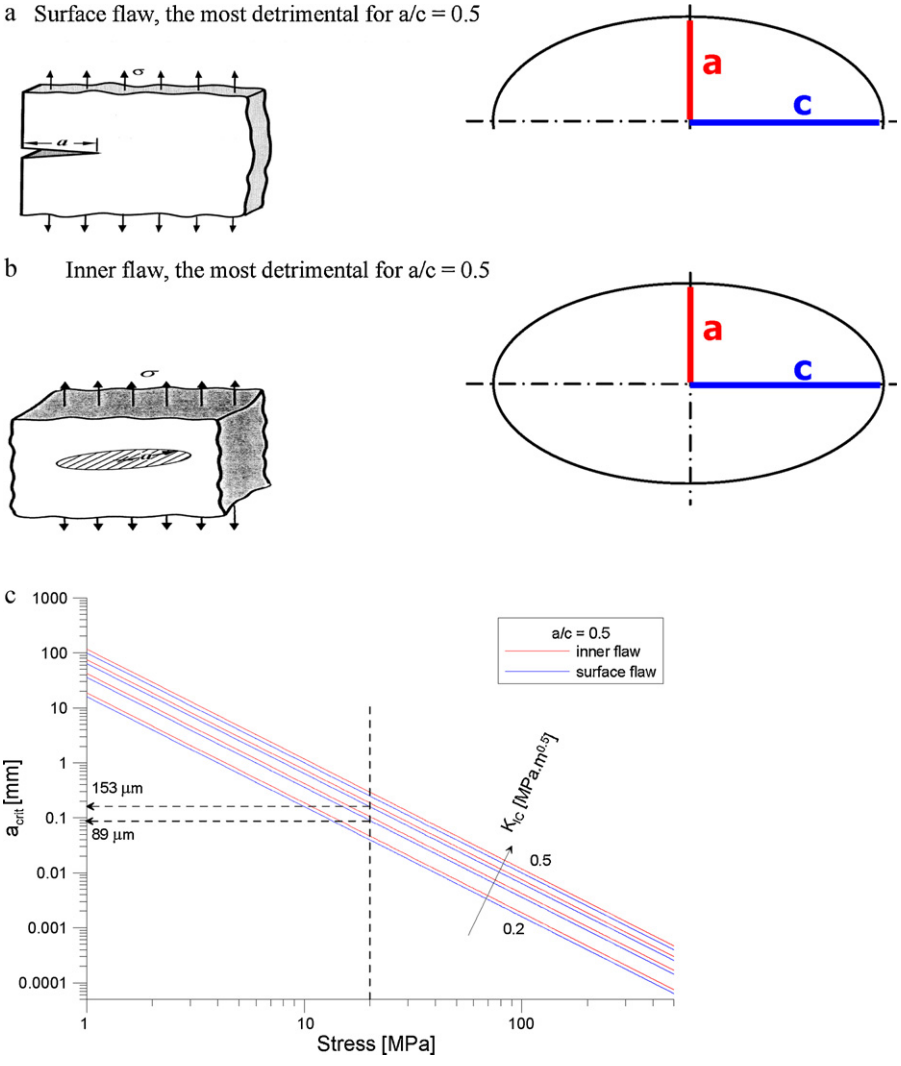

Fig. 4. Most detrimental flaw geometries: (a) surface flaw; (b) inner flaw, (c) diagram representing the flaw sizes for the applied stresses.

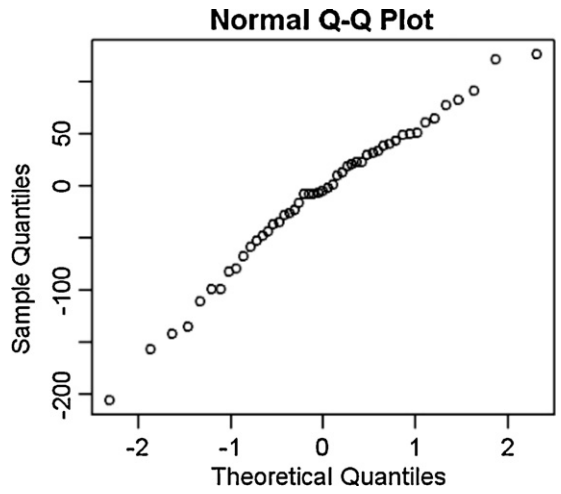

Fig. 5. q–q-plot of the differences $Y_i = y_i - g(x_i)$, $i = 1, 2, \ldots, 50$ suggesting a normal distribution obtained in R environment (http://cran.r-project.org/) for AR002 material.

Section 4.2(a) and (b). The mathematical equation (20) represents our base semi-empirical theoretical model for the calculation of mean lifetimes for the new components (of course, of the same material that will work under same service life conditions)

$$y = g(x) = 0.0011 * X^3 - 0.1672 * X^2 + 1.7805 * X + 503.54 \quad (20)$$

To verify the goodness of fit, another lot of 50 specimens was considered: $\{(x\_i, y\_i), i = 1, \ldots, 50\}$.

The differences

$$Y_i = y_i - g(x_i), \quad i = 1, 2, \ldots, 50$$

between the y values of experimental data and the model were calculated. These differences can be supposed normally distributed, as it appears quite realistic from a usual q–q-plot, obtained by R environment (http://cran.r-project.org/) and reported in Fig. 5.

Moreover, such a normality hypothesis (in statistics, the null hypothesis H_o) is successfully tested by a Kolmogorov–Smirnov normal test. The tests was performed in R environment (http://cran.r-project.org/), obtaining a p-value = 0.6418.

Notice that here the null hypothesis is normality and it would be rejected if $p < 0.05$; for $p = 0.64$ the normality holds quite true.

Once normality has been confirmed, a usual t-test on the differences $Y_i = y_i - g(x_i)$ has been performed to determine the goodness of the curve fitting (now the H_o hypothesis is $\mu = 0$). In this case, a p-value = 0.3472 is obtained, with a 0, 95% confidence interval: [−30.15134, 10.81170] and a mean: −9.66982.

First it turns out that the null hypothesis is not rejected, since $p = 0.34$ is greater than 0.05. Moreover the confidence interval of such a mean is [−30.15, 10.81]. This is a fairly strong confirmation of the goodness of the curve since mean lifetime is predicted by the model $y = g(x)$ with an absolute error of at most 30 cycles. Notice that it corresponds to a relative error of about 9%.

An estimate of the critical length below and above which a transition can be thought of, is the deflection point of the sigmoidal curve reported in Fig. 3. If the generic curve model is $y = g(x) = a * x^3 + b * x^2 + c * x + d$, hence the deflection point is $x = -b/(3a) = 50.66$ mm.

Let us select the lengths below 50.66 and perform a t-test on the mean of corresponding number of cycles. The 95% confidence interval in this case is [392.6741, 458.5673], with of mean of 425.6207. It is important to see the confidence interval of the mean: if the length is less than the critical length, the corresponding number of cycles is, in mean, greater than 392.67 and lower than 458.5673 with probability 95%.

Then selecting the lengths above 50.66 we obtain a 95% confidence interval of [139.3260, 225.1740] with a mean of 182.25 cycles. Therefore, if the path length is greater than the critical length, the lifetime is, in mean, between 139.32 and 225.17 number of cycles (with probability 95%).

The results obtained put in evidence that there is a sufficiently good fitting between absolute values predicted by the model and the real ones bearing in mind that the approach is used to estimate lifetime from parameters measured in as-received state (the relative error varies from 10 to 30%).

However, beyond the importance of this later statistical characterization of the model, the goodness of the approach can be appreciated considering Fig. 3. Let us consider a critical λ value (50.66 mm) that corresponds to the deflection point of the sigmoidal curve calculated. If we choose the samples having λ values higher than the critical λ as more prone to failure, we can see that even if significant differences exist between the absolute values of predicted lifetime with the real values, once the samples have performed 250 cycles of thermal treatment, from the 17 marked samples, 16 were broken.

5. Discussion

5.1. Determination of critical flaw from CFLT

When Eq. (8) of CFLT is used for the assessment of failure probability, the calculated λ value indicates a cumulative value representing the summation of all the small flaws that the ultrasonic wave finds along its path. However, to obtain real flaw sizes from ultrasonic velocity data obtained by UPVT technique, some considerations are necessary, as follows:

- λ represents in Eq. (8) a cumulative flaw value because the ultrasonic velocity considered as (v_0) in the equation is equal to a maximum value.
- In the case of ultrasonic velocity measured through the length of the refractory plates, it could be considered that the cumulative flaw values (λ) obtained from Eq. (11) are very close to the values of real flaw sizes (a_{real}). These real flaw sizes correspond to the macroscopic flaw propagating in the transversal direction of the refractory plates (which lead them to fracture). Macro-cracking in these materials under thermal shock is a single phenomenon observed only in the transversal direction and mostly attributable to one single crack.[7] The higher is the real flaw size, the higher is the convergence

to the theoretical cumulative value represented by (λ) and calculated by Eq. (11) of CFLT, according to Eq. (21):

$$\lambda = L\left(\frac{v_0}{v} - 1\right) \cong a_{real} \quad (21)$$

- However, to obtain microscopical real flaw sizes by CFLT using ultrasonic velocities measured through the thickness of the plates,[7] some previous considerations are required: the correct v_0 value in Eq. (11) should be the mode value (v_{mode}) of ultrasonic velocity data (instead of the maximum value as in the case of ultrasonic velocity measured through the length of the refractory plates). It could be considered that v_{mode} corresponds to a representative ultrasonic velocity through the material, and hence it is possible to assign a nil value to the corresponding cumulative value (λ_1). Therefore the difference between generic v values and v_{mode} (or respective λ and λ_1 values) represents flaw lengths beyond the mean value and hence critical flaw sizes. Hence the equation given the microscopical real flaw sizes by CFLT using ultrasonic velocities measured through the thickness of the plates is presented below:

$$\lambda = L\left(\frac{v_{mode}}{v} - 1\right) \cong a_{real} \quad (22)$$

As mentioned in Section 4.1 and discussed in detail elsewhere,[7] it can be hypothesised that the S-like curves of Fig. 1a and b represent the crack-growth rate as function of the initial length of the most critical crack present in the as-received material in the transversal direction. The remarkable similarity between the functions proposed by Baratta, Green and Evans[18–21] describing the normalized stress-intensity factor as a function of the crack length to void radius ratio with the S-like curves of as-received ultrasonic velocity data against number of industrial thermal cycles in this study (Fig. 1a and b) suggests the potential use of CFLT and LPT approaches, which are based on ultrasonic velocity measurement, as a convenient quantitative tool for fracture mechanics studies, as discuss in detail in a previous work.[7] Briefly, toughening mechanisms acting in different refractory materials have been reported by several authors, for example by Baker et al.[22] In particular crack tip blunting and viscoelastic bridging have been observed in cordierite-mullite materials as discussed elsewhere.[7] Toughened ceramics are characterized by a crack-growth resistance curve (R-curve) rather than by a single-value fracture toughness. The resistance to crack growth in such materials increases as the length of the cracks increases. It can be expected that the efficiency of viscoelastic bridging in silicate-based systems, such as the present refractory plates, can influence the linearity between stress intensity factor and crack growth rate and hence affect the characteristics of the S-like curve giving the correlation between the as-received ultrasonic velocity (or corresponding flaw lengths if Eq. (11) is applied) and the number of industrial thermal cycles (Fig. 1a and b). Assuming this fact as valid, it is possible to infer three different stages of crack-growth rate (Fig. 2), being lower for small and long cracks than for cracks of medium length, which could indicate an R-curve behaviour of the investigated materials, as discussed elsewhere.[7] When the defect present in the material is longer than the critical length, which leads to a critical ultrasound velocity v_c, as labelled in Fig. 1a and b and λ_c in Fig. 2c and d, the crack will propagate faster and as a logical consequence the service life of the materials will be short. Therefore, from the manufacturer point of view, it is more convenient to have a higher number of sub-critical cracks initially rather than just one large crack exceeding the critical length, as expected. The fact that CONC material presents a lower v_c value than AR002 material (Fig. 1) indicates that the CONC material is able to withstand the propagation of a larger initial critical crack. This in turn shows that the microstructure of the CONC refractory material should activate toughening mechanisms able to counteract during service life the effect of large manufacturing defects.

Further investigations of the ultrasonic velocity and fracture toughness correlation as well as high temperature mechanical fatigue studies of the refractory materials are being carried out to confirm this assumption. If this approach is valid, it will be possible to have a predictive tool of the complete refractory service life just by performing accurate measurements of the ultrasonic velocity in the as-fabricated samples, as proposed in this study.

5.2. Microscopical critical flaw size by CFLT and fracture mechanics: verification of the proposed method

5.2.1. Microscopical critical flaw size by CFLT and LPT

Fig. 2A shows the crack length determined by CFLT as function of the service life for the AR002 and CONC refractory materials, for ultrasonic velocity values measured through the thickness. For the assessment of flaw distribution all velocities v available along the linear thickness path were considered and $v = v_{mode}$ was used in Eq. (11). These critical flaw sizes are closed to the average values of chamotte grain dimensions (chamotte is the inert phase present in the microstructure[7]). The increasing trend of service life up to a flaw size length close to the chamotte grains length is in agreement with literature findings,[23] which showed that microcracking below the chamotte grain dimension could be helpful to improve thermal shock resistance. The critical flaw size was established at the λ mode value, since longer cracks decrease the service life. Hence, the critical flaw length values are $\lambda_c = 460\ \mu m$ and $\lambda_c = 300\ \mu m$ for AR002 and CONC materials, respectively. It is worthwhile mentioning the good agreement between these values obtained from CFLT and the average flaw length determined from Image Analysis. Moreover, the fact that CONC presents a lower critical flaw size explains the early crack initiation in this material[1,7] as indicated also by the lower Hasselman's parameter "*R*", calculated in previous works.[7]

5.2.2. Microscopical critical flaw size determination by Chevron notched (CN) specimen technique

For exact determination of the critical flaw size it is necessary to know the acting (external) load or the applied stress in the location of the flaw. If this stress is unknown it is possible to develop diagrams showing dependence of the critical flaw size a_{crit} on the applied stress σ for different levels of fracture

toughness K_{IC}, i.e. for the critical condition of catastrophic fracture. Considering Eq. (23) based on Griffith-Irwin's work:

$$K_{IC} = \sigma\beta\sqrt{a_c\pi} \quad (23)$$

where a_c is a critical crack length, β is a geometrical parameter ($\beta = 1$ for a crack centred in an infinite plate; $\beta = 1.12$ for a crack at the edge of the plate) and σ is the tensile strength ($0.6\sigma_f$), a diagram has been plotted for the two most typical flaw configurations, surface flaw and internal flaw (see Fig. 4). The most detrimental flaw geometries are shown schematically in Fig. 4a and b and for these two configurations and flaw geometries the diagrams representing the flaw sizes as function of the applied stresses are shown in Fig. 4c.

As an example, the applied stress corresponding to the flexural strength level can be selected. For the investigated composites this stress can be taken as ~20 MPa.[23] For this level of applied stress and for fracture toughness corresponding to 0.3 $MPam^{1/2}$ (e.g. CONC material) the critical flaw size is 89 μm in case of surface flaw and 102 μm in case of inner flaw. For the same applied stress and fracture toughness of 0.4 $MPam^{1/2}$ (e.g. AR002 material) the critical size of the surface flaw is 153 μm whereas the inner flaw may have the size of 185 μm.

The values of critical crack length are controlled by the value of fracture toughness. This means that the lower the fracture toughness the smaller the critical crack length (at the same applied stress). The diagrams are independent of the material. It is possible to estimate for a given level of applied stress (horizontal axis) the critical crack length (vertical axis) applying the known value of fracture toughness (corresponding curve from the diagram).

However, there is the remaining uncertainty regarding which value of applied stress should be used. This should follow from the estimation of the component loading taking into account the geometry, real forces acting on the component, etc. Table 4 shows data of critical flaw size, supposing a surface crack (more detrimental case). The first set of values are calculated for a stress corresponding to the critical fracture condition for the bending strength test. The other set is calculated for about half of this stress, i.e. for a stress of 10 MPa acting on the flaw. The second case appears to be more realistic for the service condition. The basic relation of flaw sizes for CONC and AR002 materials is the same, however AR002 appears to behave slightly better compared to CONC in the initial state ($a_c = 291$ μm and 461 μm for CONC and AR002 specimens, respectively, see Table 4). The microscopical critical flaw size values obtained from Cumulative Flaw Length Theory were 300–320 μm for CONC and 450 μm for AR002 material. They represent the initial condition for the crack. This result appears to be in very good correlation with the minimum values generated by fracture toughness determination and the critical flaw sizes calculated for the local stress of 10 MPa, which can be considered close to an effective strength value (σ_e) (strength in service) of 60% of the nominal fracture strength.

The lower value of critical flaw size of CONC material obtained from CFLT (from the ultrasonic velocity histogram) was confirmed by the critical flaw size values obtained from the destructive test (K_{IC} measurement by chevron notched specimen technique) and from image analysis. This explains the fact that CONC components present an early crack initiation in comparison to AR002 material (lower value of critical flaw size).

5.3. Macroscopic critical crack size values obtained from ultrasonic velocity measurement through the length of refractory components

The critical crack length after some crack propagation has occurred (macrostructural crack initiation) is more complicated to calculate from destructive testing, i.e. chevron notched specimen technique. It is not possible to calculate the crack size from the initiation fracture toughness measured by chevron notch or other technique. The conditions are controlled by the local stress intensity factor corresponding to the applied load but affected by local fracture mechanisms (in coarse grained microstructures there is even the possibility of local mixed mode K_I and K_{II} when a crack is deflecting around the grain boundary). Hence the macroscopical values of critical flaw size obtained from CFLT using ultrasonic velocity data through the length of the refractory plates, cannot be validated by the chevron notched specimen technique results. However, the values obtained from CFLT (50.66 and 58 mm for AR002 and CONC materials, respectively), are in good agreement with experimental data of their life service behaviour,[7] which state that CONC samples, despite showing an early crack initiation, present a slower crack propagation rate, as confirmed by the longer lifetime of CONC refractory plates (higher macroscopic critical flaw size). This fact is also indicated by the higher Hasselman's parameter

Table 4
Data of critical flaw size, assuming a surface crack (more detrimental case Fig. 4a) for CONC and AR002 materials.

	CONC		AR002	
	Lowest value of a_{crit} (μm)	Mean value a_{crit} (μm)	Lowest value a_{crit} (μm)	Mean value a_{crit} (μm)
For the applied load of 20 MPa (about flexural stress level)				
Initial state	75	119	119	155
State after 30 thermal shocks	39	46	18	75
For the applied load of 10 MPa				
Initial state	**291**	461	**461**	544
State after 30 thermal shocks	161	196	86	291

R'''' calculated in a previous work,[7] which characterizes crack propagation under thermal shock conditions.

5.4. Final considerations

Assuming that the S-like curves of Fig. 1 or Fig. 2B are the representation of the crack grow rate as function of initial length of the most critical crack present in the as-received material in transversal direction, the following can be concluded:

(i) There is a good agreement between microscopical critical flaw data obtained from fracture mechanics technique (a_c) and from CFLT using thickness ultrasonic velocity data (λ_c). The lower a_c and λ_c values of CONC material explain the early crack initiation in this material.
(ii) The values of macroscopic critical flaw size (λ_c) obtained by CFLT from measurement through the length are in agreement with experimental industrial evidence and in situ crack measurements.
(iii) The higher values of macroscopical critical flaw size of CONC material explain its better thermal shock behaviour; despite showing an early cracking initiation this material presents a lower crack propagation.

These statements indicate that single measurements of the fracture toughness in the initial state do not allow prediction of the performance of refractory materials under thermal shock conditions since this single value (K_{IC}) does not give information about the R curve behaviour of the materials. On the contrary, the determination of the microscopical and macroscopical critical flaw sizes and the S-like curves by LPT method presented in this paper allows to predict the behaviour of the materials. These S-like curves can be also confirmed by the similarity with earlier theoretical models[7] and could be related to the R curve behaviour of the materials.

Thus the main finding of this investigation is that the S-like curve, obtained by the LPT approach and based on a statistically significant number of samples, can be used to calculate the service life of refractory materials: it could be possible to estimate the future service life of a new component from ultrasonic velocity measurements carried out in the as-fabricated state, with absolute errors ranging between 10% and 30%.

6. Conclusions

In this work the capability of the ultrasonic velocity technique (UPVT) in conjunction with the Cumulative Flaw Length Theory (CFTL) for sensitive and reliable non-destructive characterization of thermal shock damage in refractory materials has been described. CFLT permits to determine flaw length distribution in ceramic materials to obtain the critical flaw size and hence to predict the failure probability for an arbitrary stress knowing the relevant failure statistics. This knowledge is fundamental for assessing structural and/or high temperature applications of ceramics. A new statistical method (LPT theory) was proposed here that, based on the results obtained from CFLT for as-fabricated samples, allows to estimate the component lifetime when the stress state applied in service and the scattering of the measured ultrasonic velocity values are known.

The remarkable similarity between the S-like curves obtained by the LPT approach, giving the correlation between ultrasonic velocity values of samples in as-fabricated state (or crack length if CFLT is applied) and number of industrial thermal cycles, and the functions proposed by Baratta, Green, Evans and Paris,[18–22,24] describing normalized stress-intensity factor as a function of the crack length to void radius ratio, suggests the potential use of ultrasonic velocity as a convenient quantitative tool for fracture mechanics studies. Moreover the values of critical flaw size obtained from this approach are in agreement with those obtained from the destructive test measurements (chevron notch technique). This fact suggests the possibility to estimate failure probability, lifetime prediction and critical flaw length from a non-destructive characterization of the material based on ultrasonic velocity measurement. This approach could be used not only in the stage of materials design and manufacture, but also to monitor the eventual increase of failure probability during the materials subjected to service life (e.g. in the case of refractory materials following thermal cycling).

Acknowledgment

I.D. would like to acknowledge financial support provided by the Czech Science Foundation under projects number 101/09/1821. D. Boccaccini wishes to thank the technical staff at the University of Modena and Reggio Emilia (Italy) for experimental support.

References

1. Boccaccini DN, Maioli M, Cannio M, Romagnoli M, Veronesi P, Leonelli C, et al. A statistical theory for the assessment of reliability in ceramic materials from ultrasonic velocity measurement: Cumulative Flaw Length Theory. *Eng Fract Mech* 2009;**76**(11):1750–9.
2. Damhof F, Brekelmans WAM, Geers MGD. Experimental analysis of the evolution of thermal shock damage using transit time measurement of ultrasonic waves. *J Eur Ceram Soc* 2009;**29**(8):1309–22.
3. Posarac M, Dimitrijevic M, Volkov-Husovic T, Majstorovic J, Matovic B. The ultrasonic and image analysis method for non-destructive quantification of the thermal shock damage in refractory specimens. *Mater Des* 2009;**30**(8):3338–43.
4. Terzić AM, Pavlović LM. Application of results of nondestructive testing methods in the investigation of microstructure of refractory concretes. *J Mater Civil Eng* 2010;**22**(9):853–7.
5. Chotard T, Soro J, Lemercier H, Huger M, Gault C. High temperature characterisation of cordierite-mullite refractory by ultrasonic means. *J Eur Ceram Soc* 2008;**28**:2129–35.
6. Briche G, Tessier-Doyen N, Huger M, Chotard T. Investigation of the damage behaviour of refractory model materials at high temperature by combined pulse echography and acoustic emission techniques. *J Eur Ceram Soc* 2008;**28**:2835–43.
7. Boccaccini DN, Romagnoli M, Veronesi P, Cannio M, Leonelli C, Pellacani G, et al. Quality control and thermal shock damage characterization of high-temperature ceramics by ultrasonic pulse velocity testing. *Int J Appl Ceram Technol* 2007;**4**(3):260–8.
8. Chen ES, Buyokozturk O. Methodology for thermomechanical analysis of brittle systems. *Am Ceram Soc Bull* 1985;**64**(7):982–8.

9. Buyukozturk O, Tseng TM. Thermomechanical behavior of refractory concrete linings. *J Am Ceram Soc* 1982;**65**(6):301–7.
10. Harmuth H, Tschegg EK. Fracture mechanical characterisation of ordinary ceramic refractory materials. *Veitsch-Radex Rundschau* 1994;**1–2**:465–80.
11. Bell A. A computer simulation of cracking in monolithic refractories. *Brit Ceram Trans J* 1988;**87**.
12. Damhof F, Brekelmans WAM, Geers MGD. Non-local modelling of cyclic thermal shock damage including parameter estimation. *Eng Fract Mech* 2011;**78**(9):1846–61.
13. Gils MAJ, Dortmans LJMG, With G, Brekelmans WAM, Vree JHP. Size effect predictions by fracture models for a refractory ceramic. *Int J Fract* 1996;**75**:273–83.
14. Hasselman DPH. Unified theory of thermal shock fracture initiation and crack propagation in brittle materials. *J Am Ceram Soc* 1969;**52**(11):600–4.
15. Kingery WD, Bowen HK, Uhlmann DR. *Introduction to ceramics*. 2nd ed. New York: J. Wiley & Sons; 1976. p. 540.
16. Bradt RC. Fracture of refractories. *Mechanical engineering. Refractories handbook*, vol. 178. Marcel Dekker; 2004. p. 11–38.
17. Bluhm JI. Slice synthesis of a three-dimensional work of fracture specimen. *Eng Fract Mech* 1975;**7**:593–604.
18. Baratta FI. Stress intensity factor estimates for a peripherally cracked spherical void and a hemispherical surface pit. *J Am Ceram Soc* 1978;**61**: 490–3.
19. Evans AG, Biswas DR, Fulrath RM. Some effects of cavities on the fracture of ceramics: 11, spherical cavities. *J Am Ceram Soc* 1979;**62**(2):101–6.
20. Green DJ. Stress intensity factor estimates for annular cracks at spherical voids. *J Am Ceram Soc* 1980;**63**:342–4.
21. Baratta FI, Parker AP. Mode I stress intensity factor estimates for various configurations involving single and multiple cracked spherical voids. In: Bradt RC, Evans AG, Hasselman DPH, Lange FF, editors. *Fracture mechanics of ceramics*, vol. 5. Plenum Press; 1983. p. 543.
22. Baker T, Zimba J, Akpan E, Bashir I, Watola C, Soboyejo W. Viscoelastic toughening of aluminosilicate refractory ceramics. *Acta Mater* 2006;**54**:2665–75.
23. Aksel C, Warren PD. Thermal shock parameters [R, R' and R] of magnesia-spinel composites. *J Eur Ceram Soc* 2003;**23**(2):301–8.
24. Paris P, Erdogan F. A critical analysis of crack propagation laws. *J Basic Eng Trans Am Soc Mech Eng* 1963;**85**:528–34.